

# Research on convective heat transfer mechanism of a rough single fracture in granite

Bo Zhang<sup>1</sup>, Yanlong Li<sup>1\*</sup>, Tiankui Guo<sup>2</sup>, Nengyou Wu<sup>1,3</sup>, Zhanqing Qu<sup>2</sup>

1 Laoshan laboratory, Qingdao, 266237, China

2 School of Petroleum Engineering, China University of Petroleum (East China), Qingdao, 266580, China

3 Key Laboratory of Gas Hydrate, Ministry of Natural Resources, Qingdao Institute of Marine Geology, Qingdao, 266237, China

## ABSTRACT

Hot dry rock (HDR) is a deep geothermal resource with great potential and is clean and environmentally friendly. During HDR exploitation, it is necessary to form a penetrating heat transfer channel. Therefore, heat transfer in thermal reservoir has an important influence on the heat extraction of HDR. The rough single fracture is obtained by means of Brazilian splitting test, and the point-cloud data on the rough fracture is acquired by 3D laser scanner. The 2D rough single fracture convective heat transfer model is established by numerical simulation to analyze the convective heat transfer characteristics and carry out the Morris global sensitivity analysis. The results show that the outlet temperature and average heat transfer coefficient increase with the roughness increasing, and the local heat transfer coefficient is strongly correlated with the undulating and fluctuating degree. The increase of the average and local heat transfer coefficient is more obvious when the fracture aperture is larger ( $>40\mu\text{m}$ ) or initial flow rate is higher ( $>50\text{mm/s}$ ). This study can provide scientific basis for engineering design of enhanced geothermal systems.

**Keywords:** Geothermal energy; Hot dry rock; Rough fracture; Numerical simulation; Heat transfer coefficient

## NONMENCLATURE

### Abbreviations

EGS	Enhanced Geothermal System
HDR	Hot Dry Rock
JRC	Joint Roughness Coefficient

### Symbols

$Z_2$	Root mean square
$n$	Sampling point number
$u$	Flow rate
$\rho_f$	Fluid density
$p$	Fluid pressure
$\mu$	Dynamic viscosity of fluid
$C_f$	Specific heat capacity of fluid
$\lambda_f$	Thermal conductivity of fluid

$T_f$	Fluid temperature
$\lambda_r$	Thermal conductivity of rock
$T_r$	Rock temperature
$v_{in}$	Initial flow rate
$p_{out}$	Outlet pressure
$T_{ini}$	Initial fluid temperature
$T_c$	Outer wall temperature
$T_0$	Initial rock temperature
$Q$	Heat exchange
$q_f$	Volume flow rate
$T_{in}$	Inlet temperature
$T_{out}$	Outlet temperature
$h$	Average convective heat transfer coefficient
$T_f$	Average fluid temperature in fracture
$T_r$	Average rock temperature at fracture surface

## 1. INTRODUCTION

Geothermal resource is a clean and renewable energy with the manifold advantages such as wide distribution, large reserves and free from weather restrictions, which can solve the environmental problems caused by the massive use of fossil fuels and meet the increasing energy demand. Hot Dry Rock (HDR) is usually located 3-10km below the surface of earth, with large reserves and high temperature. However, due to its characteristics of low porosity and low permeability, its utilization rate is low<sup>[1]</sup>. In order to exploit the heat energy in HDR, artificial stimulation<sup>[2,3]</sup> is needed to reconstruct the reservoir to form a fracture channel between the injection well and the production well to enhance the reservoir's conductivity. Such projects used for geothermal exploitation are called enhanced geothermal systems (EGS)<sup>[4]</sup>. Therefore, convective heat transfer between the flowing fluid and the rock fracture is one of the key scientific issues involved in EGS. It is of great significance for the design and evaluation of EGS stability to accurately understand the convective heat transfer characteristic of the fluid in

the fracture channel during the heat energy extraction process in HDR.

For rock masses where natural joints are not developed, the flow of fluid in the reservoir is dominated by the single fractures such as faults<sup>[5,6]</sup>. Moreover, the process of convective heat transfer in multi-fractures is more complex. Therefore, studying convective heat transfer characteristics in single fractures is the basis for studying heat transfer characteristics in multi-fractures. In order to analyze problems conveniently, some scholars study the convective heat transfer process mainly based on the smooth and horizontal single fracture<sup>[7,8]</sup>. Pruess (1983) studied the transient equilibrium problem of heat transfer between a porous rock matrix and fractures, and obtained the analytical solution of convective heat transfer between bedrock and fractures<sup>[9]</sup>. Mohais et al. (2011) present an analysis of fluid flow and heat transfer through a single horizontal channel with permeable walls which are at different temperatures<sup>[10]</sup>. However, both natural fractures and artificially stimulated fractures usually have rough surfaces. Thereby, some scholars conducted experimental studies on the convective heat transfer characteristics of rough single fractures. Zhao and Tso (1993) used conducted 78 groups of convective and heat transfer experiments of rough single fractures based on cylindrical rock samples with a diameter of 51mm and a height of 102mm, and obtained accurate and abundant experimental data<sup>[11]</sup>. Li et al. (2017) carried out a series of convective and heat transfer experiments for artificial smooth and rough single fractures of sandstone and granite, and studied the effect of fracture surface roughness on heat transfer intensity<sup>[12]</sup>. Bai et al. (2017) carried out convective heat transfer experiments for single fractures of granite under different temperatures and confining pressures to study the correlation between the overall convective heat transfer coefficient and fracture opening and flow rate<sup>[13]</sup>. Ma et al. (2018) used 3D printing technology to create different rough single fractures and studied the convective heat transfer characteristics of roughness and tortuosity to single fractures in granite<sup>[14]</sup>. These experimental researches have improved people's understanding of the characteristics of convective heat transfer in a single fracture of rock. However, due to the limitations of experimental conditions, it is difficult to measure the temperature or fluid flow rate of each position along the fluid flow direction of the fracture surface, which cannot reflect the local heat transfer characteristics. Therefore, a few scholars carried out numerical simulation studies. By means of the experimental data of Zhao and Tso (1993)<sup>[11]</sup>, Zhao (2014) carried out numerical simulation

research and obtained the analytical solution of the fluid temperature distribution along the fracture surface in the convective heat transfer process of single fracture granite<sup>[15]</sup>. Based on the 10 standard roughness curves proposed by Barton (1973) in 1973<sup>[16]</sup>, He et al. (2019) studied the influence of rough single fracture morphology in granite on convective heat transfer characteristics, and proposed a morphological condition factor to quantify the influence of fracture morphology on convective heat transfer characteristics<sup>[17]</sup>. Nevertheless, the convective heat transfer process between fluid and fracture is affected by many factors, such as fracture opening, fluid type, rock and fluid thermophysical properties, fracture morphology, fracture roughness and fluid dynamics characteristics, etc.<sup>[18-20]</sup>. Additionally, the fracture opening and permeability under the effect of temperature can also change, and further affects the convective heat transfer process. Therefore, the processes involved are complex. Although some research has been studied, there exists not a still thorough understanding of convective heat transfer mechanism even for the case of a single fracture of the granite specimen.

In this study, granite is selected as the research object and water is chosen as working fluid. Then, the rough single fracture is obtained by the Brazilian splitting test, and a 2D convective heat transfer model based on the obtained rough single fracture curve is established to analyze the influence of fracture opening and initial flow rate on the convective heat transfer characteristics. And the evolution of average convective heat transfer coefficient and local convective heat transfer coefficient under different roughness are analyzed. Finally, Morris global sensitivity analysis method is used to analyze the influence of fracture opening, initial fluid flow rate, specific heat capacity of fluid, specific heat capacity of rock mass, thermal conductivity of fluid and thermal conductivity of rock mass on outlet temperature and average convective heat transfer coefficient, which can provide scientific basis for EGS engineering design.

## 2. NUMERICAL MODEL AND SIMULATION

### 2.1 2D convective heat transfer model

The fracture opening in HDR reservoirs is extremely narrow, normally in microns or millimeters<sup>[21]</sup>. It is difficult to investigate the local convective heat transfer characteristics between fractures and surrounding rocks by experimental methods. However, numerical simulation can solve this problem, but the rationality of the simulated data needs to be verified. Therefore, in order to verify the numerical simulation results and the

subsequent analysis of convection heat transfer characteristics, a 2D single fracture model with a length of 102mm in the x direction and 51mm in the Y direction was established according to the rock size used by Zhao and Tso (1993)<sup>[11]</sup>, as shown in Fig. 1, and the following assumptions are made.

(1) The rock is regarded as isotropic material and its permeability is ignored and the rock, that is, water flows only in the fracture.

(2) The water flow in the fracture is stable laminar flow, incompressible Newtonian fluid, and the physical parameters are constant.

(3) The heat radiation is ignored in the heat transfer process.

(4) Water migrates in liquid, regardless of the phase transition of water.

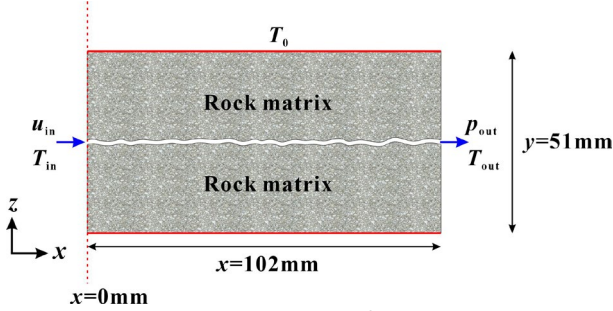


Fig. 1. Schematic diagram of two-dimensional convective heat transfer.

## 2.2 Rough fracture acquisition

In this study, the Brazilian splitting experiment was used to construct a real rough fracture surface. Granite specimens were obtained from a mining area in Suizhou city in Hubei province, China, which was gray at a mining depth of approximately 200m, and they were gray-white. X-ray diffraction (XRD) showed that the main mineral components were albite (77.68%), quartz (10.58%) and muscovite (6.28%), with an average density of 2.60g/cm<sup>3</sup>. To avoid the ending effect, cubic rock specimens of 100mm×100mm×120mm were prepared. As shown in Fig. 2, the RFP-03 mechanical testing machine was used to carry out the Brazilian splitting experiment, and then Freescan X5 3D laser scanner was used for 3D laser scanning analysis. Thereafter, the point cloud data were obtained every 5mm in the width direction of fracture surface and 9~111mm in the direction of length. Then the point cloud data was imported into the Geomagic software and used for data processing. Finally, the processed point cloud data was imported into Auto CAD to generate the rough fracture curves, and five roughness curves numbered b ~ f shown in Fig. 3 were selected for subsequent numerical simulation analysis.

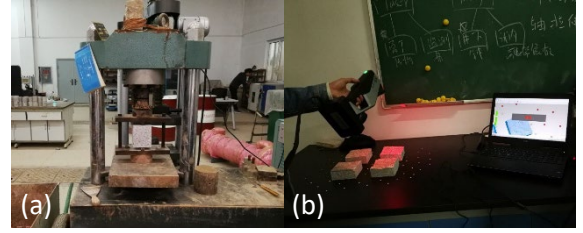


Fig. 2. Brazilian experiment and 3D laser scanning analysis. (a) Brazilian splitting test. (b) 3D laser scanning analysis.

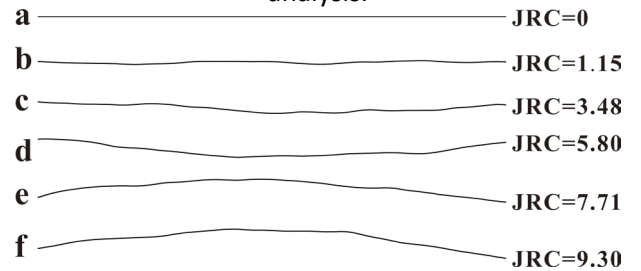


Fig. 3. Rough profile curves with different degrees of roughness.

In order to study the effect of roughness on convective heat transfer of a single fracture in granite, joint roughness coefficient (JRC) is used to characterize the roughness of the fracture. According to previous studies<sup>[22]</sup>, JRC is calculated as follows:

$$JRC = -4.41 + 64.46 \cdot Z_2 \quad (1)$$

Where,  $Z_2$  represents the root mean square of the first derivative, and the calculation Eq. (2) is as follows:

$$Z_2 = \left[ \sum_{i=1}^{n-1} \frac{(z_{i+1}-z_i)^2}{(x_{i+1}-x_i)^2} \right]^{1/2} \quad (2)$$

Where,  $n$  represents the number of sampling points along the x direction of the entire fracture, mm.  $z_{i+1}-z_i$  represents the z-coordinate difference of adjacent sampling points and reflects the undulating degree of fracture, mm.  $x_{i+1}-x_i$  represents the x-coordinate difference of adjacent sampling points, mm. After calculation, the JRC corresponding to the five curves are respectively 1.15, 3.48, 5.80, 7.71 and 9.30, as shown in Fig. 3.

## 2.3 Governing equations

In this paper, by means of COMSOL Multiphysics, a commercial finite element software, the steady state process of convective heat transfer in which the fluid flows through a rough single fracture in granite is studied. The water flow is controlled by the continuity equation, the Navier-Stokes equation and the energy conservation equation under steady state conditions.

$$\nabla \cdot \mathbf{u} = 0 \quad (3)$$

$$\rho_f \mathbf{u} \cdot \nabla \mathbf{u} = -\nabla p + \nabla \cdot (\mu (\nabla \mathbf{u} + (\nabla \mathbf{u})^2)) - \frac{2}{3} \mu (\nabla \cdot \mathbf{u}) \mathbf{I} \quad (4)$$

$$\rho_f C_f \mathbf{u} \cdot \nabla T_f = \nabla \cdot (-\lambda_f \nabla T_f) \quad (5)$$

Where,  $u$  is flow rate, m/s.  $\rho_f$  is fluid density, kg/m<sup>3</sup>.  $p$  is fluid pressure, Pa.  $\mu$  is dynamic viscosity of fluid, Pa·s.  $\mathbf{I}$ , unit tensor.  $C_f$  is specific heat capacity of fluid, J/(kg·K).  $\lambda_f$

is thermal conductivity of fluid, W/(m·K).  $T_f$  is fluid temperature, K.

The energy conservation equation in rock under steady state is shown as follows:

$$\nabla \cdot (-\lambda_r \nabla T_r) = 0 \quad (6)$$

Where,  $\lambda_r$  is thermal conductivity of rock, W/(m·K).  $T_r$  is rock temperature, K.

#### 2.4 Initial and boundary conditions

In the EGS projects, water is a common working fluid. Thus, this study simulates the convective heat transfer process when the water flows through the rough single fracture of the granite. For the flow field, the initial flow rate is  $v_{in}$ , the outlet pressure ( $p_{out}$ ) is set at 1 atmosphere, and the upper and lower boundary of the rock is regarded as the no-flow and no-slip boundary. For the temperature field, the initial fluid temperature ( $T_{ini}$ ) is 20°C, the outer wall temperature ( $T_c$ ) and the initial rock temperature ( $T_0$ ) are set as 90°C, and the left and right boundary of the rock are set as the adiabatic boundary. The thermophysical parameters of the rock used in the simulation are derived from the thermophysical parameters of the granite used in the Brazil splitting test, as shown in Table 1. Different fracture aperture and injection flow rate are selected to study the influence mechanism on convective heat transfer. The calculation parameters under different simulation conditions are shown in Table 2.

Table 3. Model parameters and validation results.

Case number	$T_s$ (°C)	$d$ ( $\mu$ m)	$v_{in}$ (mm/s)	$T_{in}$ (°C)	$T_{out}$ (°C)	
					Experimental results	Simulation results
1	100	15.85	128.2	59	95	98.14
2	100	15.85	102.57	60	96	99.03
3	120	16.72	84.17	57	117	118.92
4	120	16.72	119.71	64	117	117.5
5	120	12.45	167.6	56	117	117.01
6	120	12.45	203.72	55	117	115

The relative deviation between the experimental value and the simulated value of outlet temperature was calculated. The maximum value of the relative deviation is 3.31%, and the minimum value is 0.01%, all of which are controlled within 5%. As for the source of error, on the one hand, the experimental study is three-dimensional, while the numerical simulation is two-dimensional. On the other hand, we assume that the physical parameters of water do not change with temperature, while in reality, the physical parameters of water can change with temperature rising. In addition,

Table 1. Parameters required for numerical simulation.

Thermophysical parameters	values
$\lambda_r$	3.46 W/(m·K)
$\rho_r$	2645 kg/m <sup>3</sup>
$C_r$	850 J/(kg·K)
$\rho_f$	1000 kg/m <sup>3</sup>
$C_f$	4200 J/(kg·K)
$\mu$	0.001 Pa·s
$\lambda_f$	0.664 W/(m·K)

Table 2. Parameters under different working conditions.

Simulation parameters	values			
Aperture ( $d$ )/ $\mu$ m	20	30	40	50
Initial flow ( $v_{in}$ )/(m/s)	10	30	50	70

#### 2.5 Model Validation

Before the simulation study, the established numerical model should be verified. In this paper, six sets of data were selected from the experiment conducted by Zhao and Tso (1993)<sup>[11]</sup>, and the same parameters were used for simulation to verify the model by comparing the outlet temperature. The parameters and results are shown in Table 3.

the water may undergo phase transitions when the temperature exceeds 100°C.

#### 2.6 Data processing

##### 2.6.1 Average convective heat transfer coefficient

The convective heat transfer coefficient is usually used to characterize the heat transfer capacity between fluid and fracture surface. In order to understand the overall heat transfer situation of different rough single fracture from a macroscopic perspective, the average convective heat transfer coefficient was used to characterize the heat transfer performance in the

fracture channel. The heat exchange between the fluid flowing through the fracture and the rock can be expressed by the following Eq. (7).

$$Q = C_f q_f \rho_f (T_{in} - T_{out}) \quad (7)$$

Where,  $q_f$  is volume flow rate,  $m^3/s$ .  $T_{in}$  is the inlet temperature, K.  $T_{out}$  is the outlet temperature, K. In addition, according to Newton's law of cooling, the heat exchange between fluid and rock at the fracture surface can be calculated, as shown in the following Eq. (8).

$$Q = hA(T_f - T_r) \quad (8)$$

Where,  $h$  is the average convective heat transfer coefficient,  $W/(m^2 \cdot K)$ .  $A$  is the heat transfer area,  $m^2$ .  $T_f$  is the average fluid temperature in fracture, K.  $T_r$  is average rock temperature at fracture surface, K. Combining Eqs. (7) and (8), the average convective heat transfer coefficient is expressed as follows.

$$h = \frac{C_f u d \rho_f (T_{in} - T_{out})}{2L(T_f - T_r)} \quad (9)$$

### 2.6.2 Local convective heat transfer coefficient

Due to the limitation of the experiment, it is impossible to know the fluid flow rate and rock temperature distribution along the fracture surface. Numerical simulation can make up for this shortcoming.

The rock can be discretized along the fluid flow direction to calculate the local convective heat transfer coefficient. The length of discretized element is  $L_i$ , and  $x_1$  and  $x_2$  are the ends of the element along the x-coordinate. If the  $L_i$  is relatively small, then the convective heat transfer coefficient is close to the convective heat transfer coefficient at a point. Eq. (10) is discretized as follows.

$$h' = \frac{C_f u d \rho_f (t_2 - t_1)}{2(x_2 - x_1)(T_i - \frac{t_1 + t_2}{2})} \quad (10)$$

Where,  $t_1$  and  $t_2$  are the temperature of two adjacent point of fluid along the flow direction.  $T_i$  is the arithmetic mean temperature of the fracture inner surface in the  $x_1$  to  $x_2$  segment.

## 2.7 Results and discussion

### 2.7.1 Temperature field

The results of the influence of fracture aperture and initial flow rate on convective heat transfer of rough single fracture are shown in Table 4. The temperature field distribution in different cases presents a similar revolution. The contour map of temperature field with roughness of 0 and 9.3 under different aperture and initial flow rate is only shown in Fig. 4.

Table 4. Numerical simulation parameters and results.

Case Number	Initial flow rate (mm/s)	Aperture ( $\mu m$ )	Average convective heat transfer coefficient ( $W/(m^2 \cdot K)$ )						Outlet temperature ( $^{\circ}C$ )					
			a	b	c	d	e	f	a	b	c	d	e	f
1	50	20	223.31	223.95	226.53	230.43	236.13	238.37	88.873	88.87	88.89	88.92	88.96	88.98
2		30	396.83	403.11	407.31	420.73	451.93	456.66	87.424	87.45	87.48	87.54	87.68	87.70
3		40	620.61	623.09	633.24	670.77	754.18	768.19	85.433	85.44	85.47	85.60	85.82	85.86
4		50	830.71	841.31	895.75	925.31	1163.08	1198.5	82.901	82.93	83.06	83.13	83.55	83.60
5	10	40	72.19	72.36	72.62	72.98	73.53	73.81	89.776	89.77	89.78	89.78	89.79	89.79
6	30		290.19	290.93	295.52	300.45	314.60	317.38	88.389	88.39	88.42	88.45	88.53	88.55
7	50		620.61	623.09	633.24	670.77	754.18	768.19	85.433	85.44	85.47	85.60	85.82	85.86
8	70		1034.18	1041.5	1077.66	1185.6	1489.92	1542.9	81.445	81.46	81.53	81.71	82.08	82.13

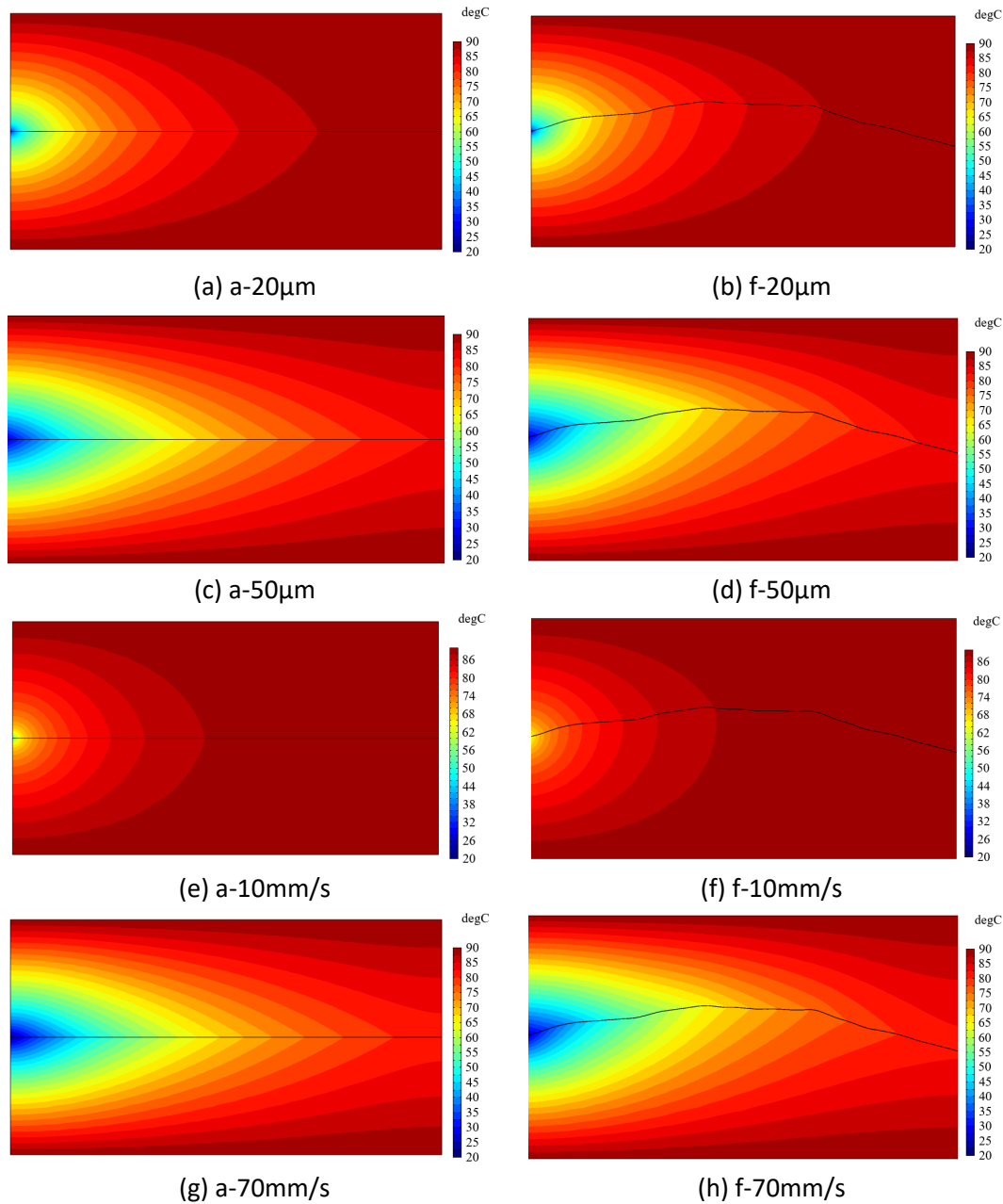


Fig. 4. Contour map of temperature field under different roughness, fracture aperture and initial flow rate.

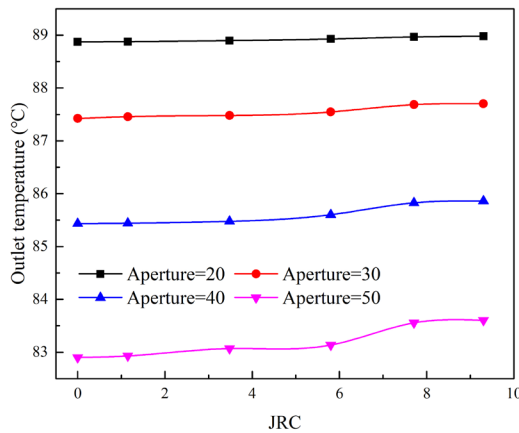
With the injection of low-temperature water, the convective heat transfer between rock and water occurs, the fracture temperature decreases, and the cold front gradually expanded to the outer wall of the rock. The rock temperature around the inlet decreases rapidly and the heat absorbed by water decreases gradually. Therefore, a banding low-temperature zone is formed and extends consistently to the outlet. And the shape changes with the fracture undulation. When the aperture or initial flow rate is fixed, the heat transfer length of the rough fracture is longer than that of the smooth and horizontal single fracture and the contour map of temperature near the outlet is sparser, indicating that the water temperature in the rough fracture is

higher than that in the smooth and horizontal single fracture. Additionally, the influence area of the low-temperature domain is larger in the concave side of the fracture surface than in the convex side, which is due to the fact that the f fracture is close to the upper wall and can be compensated in a timely manner. Under the same roughness, the larger the fracture aperture or initial flow rate is, the larger the low-temperature domain expansion area is, which is mainly attributed to the larger the fracture aperture or initial flow rate is, and more low-temperature water flows into the fracture for heat transfer.

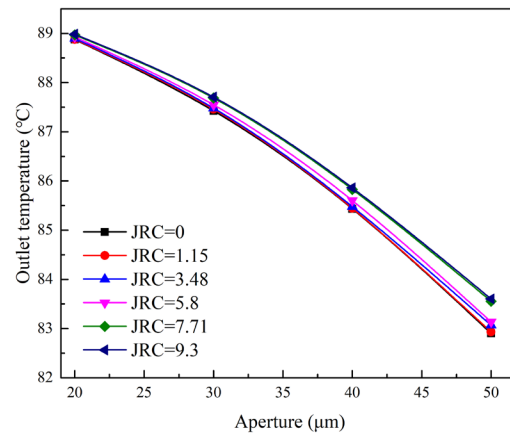
In Fig. 5(a) and (c), the outlet temperature increases slowly with the increase of roughness, which is mainly

attributed to the longer heat transfer length of the rough fracture compared with the smooth and horizontal fracture, so the water temperature heated by the surrounding rock is higher. It is worth mentioning that when the flow rate is greater than 50mm/s, the outlet temperature has a significant increase when the roughness is greater than 5.8. By comparing the fractures in Fig. 3, it can be seen that the main reason is that the overall undulation of e and f fracture is larger, and the heat transfer length is significantly higher than that of other fractures. This also indicates that increasing fracture roughness as much as possible in EGS projects is profitable to obtain higher water temperatures from production wells. In Fig. 5(b) and (d), when the initial flow

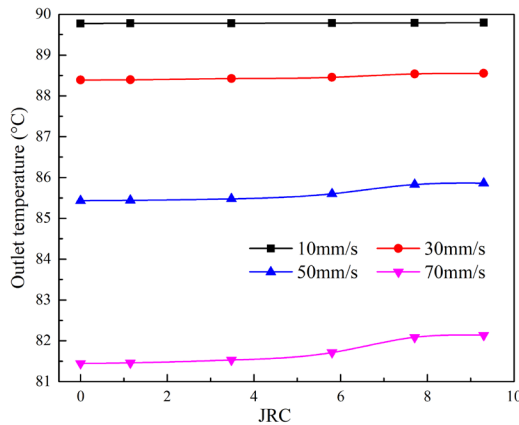
rate increases from 10mm/s to 30mm/s, the outlet temperature drops slightly. Because the flow rate is slower, the volume flow of water is lower. As the water flows along the fracture, it continuously exchanges heat with the fracture, and finally forms a heat balance with the fracture near the outlet so that the outlet temperature is basically unchanged. However, the initial flow rate changes ranging from 30mm/s to 50mm/s, the outlet temperature drops significantly due to the fact that a higher flow rate brings more volume flow of water. The heat supplies to the fracture by heat conduction is lower than the heat lost by convective heat transfer. Therefore, some water may not be fully heated, resulting in low outlet temperature.



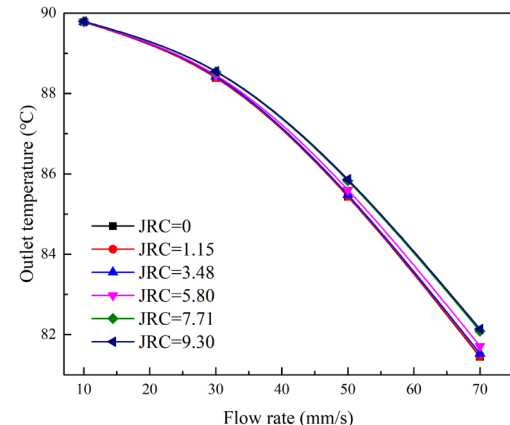
(a) Outlet temperature vs. JRC under different apertures.



(b) Outlet temperature vs. Aperture under different JRCs.



(c) Outlet temperature vs. JRC under different initial flow rates.



(d) Outlet temperature vs. Flow rate under different JRCs.

Fig. 5. Outlet temperature under different roughness, fracture apertures and initial flow rates.

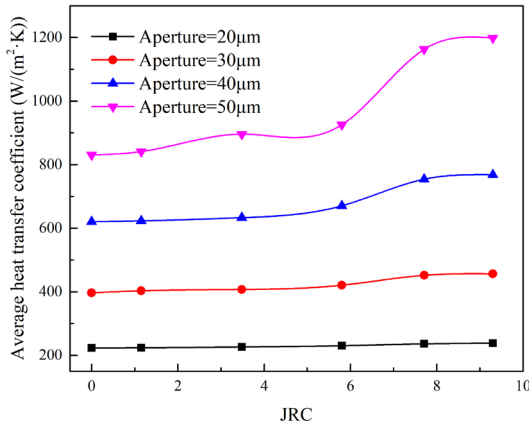
### 2.7.2 Average heat transfer coefficient

In Fig. 6(a) and (c), the average convective heat transfer coefficient increases with the increase of roughness, and when the roughness is greater than 5.8, it significantly increases, which is also attributed to the longer heat transfer length of rough fractures and the stronger convective heat transfer compared with the

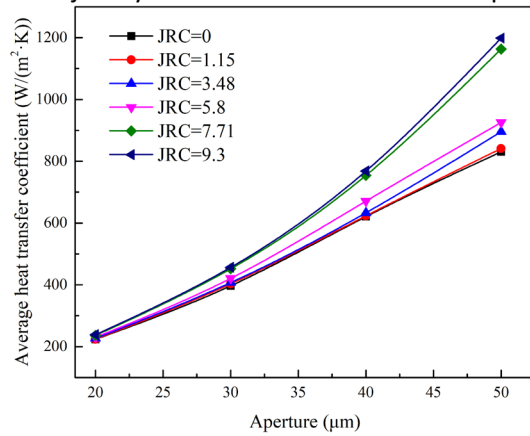
smooth and horizontal single fracture. In Fig. 6(b) and (d), the average convective heat transfer coefficient increases exponentially with the increase of fracture aperture or initial flow rate, which is mainly attributed to the wider the fracture aperture is or the faster initial flow rate is, the more the volume flow of water is used for heat transfer. However, according to the analysis in

Section 2.7.1, some water may not be fully heated, resulting in the decrease of outlet temperature with the increase of fracture aperture or initial flow rate. This indicates that it is inaccurate to rely only on outlet

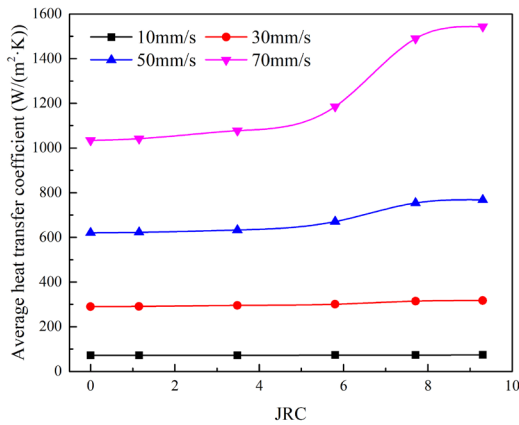
temperature or average convective heat transfer coefficient as thermal extraction efficiency index, and the outlet temperature and average should be combined to jointly evaluate thermal extraction performance.



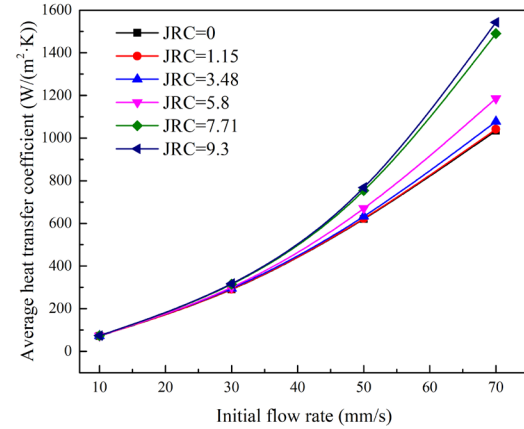
(a) Average heat transfer coefficient vs. JRC under different apertures.



(b) Average heat transfer coefficient vs. JRC under different JRCs.



(c) Average heat transfer coefficient vs. JRC under different initial flow rates.



(d) Average heat transfer coefficient vs. JRC under different JRCs.

Fig. 6. Average heat transfer coefficient under different fracture roughness, apertures and initial flow rates.

### 2.7.3 Local heat transfer coefficient

As is shown in Fig. 7, the distribution curve of local convective heat transfer coefficient fluctuates along the fracture and has a strong correlation with the fracture undulating degree. The distribution curve of convective heat transfer coefficient also shows similar evolutions in the position where the fracture undulation changes dramatically. With the increase of fracture aperture and initial flow rate, the convective heat transfer coefficient also increases obviously. It is worth mentioning that the convective heat transfer coefficient near the outlet shows a noticeable increase when the fracture aperture is wider than  $40\mu\text{m}$  or the initial flow rate is faster than  $50\text{mm/s}$ . The reason is that when closer to the outlet, the denser wave peaks are and the distribution curve of undulating degree shows an upward trend, which reveals that the fracture fluctuates and undulates dramatically. That is, the local roughness is higher, so the heat transfer efficiency is improved.

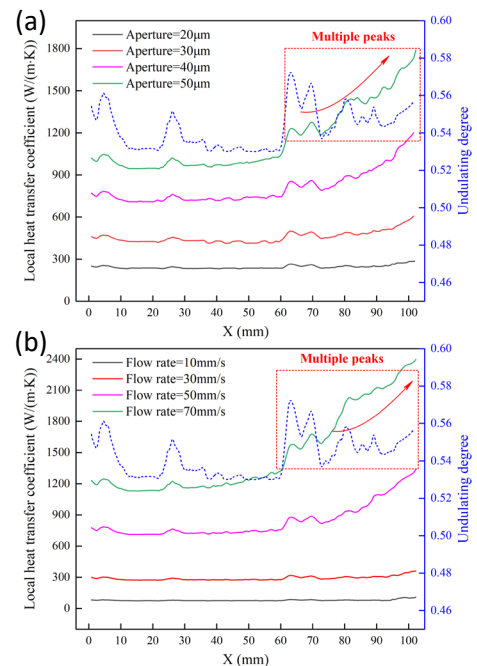


Fig. 7. Distribution diagram of the local convective heat transfer coefficient and fracture undulating degree along x direction under different fracture apertures (a) and initial flow rates (b).

As is shown in Fig. 7, the distribution curve of local convective heat transfer coefficient fluctuates along the fracture and has a strong correlation with the fracture undulating degree. The distribution curve of convective heat transfer coefficient also shows similar evolutions in the position where the fracture undulation changes dramatically. With the increase of fracture aperture and initial flow rate, the convective heat transfer coefficient also increases obviously. It is worth mentioning that the convective heat transfer coefficient near the outlet shows a noticeable increase when the fracture aperture is wider than 40 $\mu$ m or the initial flow rate is faster than 50mm/s. The reason is that when closer to the outlet, the denser wave peaks are and the distribution curve of undulating degree shows an upward trend, which reveals that the fracture fluctuates and undulates dramatically. That is, the local roughness is higher, so the heat transfer efficiency is improved.

## 2.8 Conclusions

In this paper, the rough fracture was acquired by Brazil splitting test and the cloud data of the fracture surface was obtained by 3D laser scanner. Utilizing the numerical simulation software COMSOL, a 2D numerical model of the rough single fracture in granite was established to analyze the influences of fracture aperture and initial flow rate on the convective heat transfer characteristics. The key findings are as follows: Outlet temperature and average convective heat transfer coefficient increase with the increase of fracture roughness. Especially when the fracture opening is wider than 40  $\mu$ m or the initial flow rate is faster than 50mm/s, the outlet temperature and the average convective heat transfer coefficient increase more significantly with the fracture roughness (> 5.8). The distribution curve of local convective heat transfer coefficient fluctuates along the fracture and has a strong correlation with the fracture undulating degree. The local convective heat transfer coefficient increases more obviously when the fracture aperture is wider than 40 $\mu$ m or the initial flow rate is faster than 50mm/s. To sum up, the heat transfer of the water and the fracture is stronger, and the convective heat transfer coefficient is larger, but the corresponding outlet temperature is probably lower. It is of utmost importance that the outlet temperature and convective heat transfer coefficient should be combined to jointly evaluate thermal extraction performance.

## ACKNOWLEDGEMENTS

The authors would like to acknowledge the financial support of the Shandong Postdoctoral Science Foundation (SDZZ-ZR-202501168).

## REFERENCE

- [1] Tester, J.W., Anderson, B.J., Batchelor, A.S., Blackwell, D.D., DiPippo, R., Drake, E.M., Garnish, J., Livesay, B., Moore, M.C., Nichols, K., 2007. Impact of enhanced geothermal systems on US energy supply in the twenty-first century. *Philosophical Transactions of the Royal Society A: Mathematical, Physical and Engineering Sciences* 365 (1853), 1057-1094, doi:10.1098/rsta.2006.1964
- [2] AbuAisha, M., Loret, B., Eaton, D., 2016. Enhanced Geothermal Systems (EGS): Hydraulic fracturing in a thermo-poroelastic framework. *Journal of Petroleum Science and Engineering* 146, 1179-1191, doi:10.1016/j.petrol.2016.07.027
- [3] Cheng, Y., Zhang, Y., Yu, Z., Hu, Z., Yang, Y., 2020. An investigation on hydraulic fracturing characteristics in granite geothermal reservoir. *Engineering Fracture Mechanics* 237, 107252, doi:10.1016/j.engfracmech.2020.107252
- [4] Tomac, I., Sauter, M., 2018. A review on challenges in the assessment of geomechanical rock performance for deep geothermal reservoir development. *Renewable and Sustainable Energy Reviews* 82, 3972-3980, doi:10.1016/j.rser.2017.10.076
- [5] Llanos, E.M., Zarrouk, S.J., Hogarth, R.A., 2015. Numerical model of the Habanero geothermal reservoir, Australia. *Geothermics* 53, 308-319, doi:10.1016/j.geothermics.2014.07.008
- [6] Guo, B., Fu, P., Hao, Y., Peters, C.A., Carrigan, C.R., 2016. Thermal drawdown-induced flow channeling in a single fracture in EGS. *Geothermics* 61, 46-62, doi:10.1016/j.geothermics.2016.01.004
- [7] Ghassemi, A., Nygren, A., Cheng, A., 2008. Effects of heat extraction on fracture aperture: A poro-thermoelastic analysis. *Geothermics* 37 (5), 525-539, doi:10.1016/j.geothermics.2008.06.001
- [8] Ranjith, P.G., 2010. An experimental study of single and two-phase fluid flow through fractured granite specimens. *Environmental Earth Sciences* 59 (7), 1389-1395, doi:10.1007/s12665-009-0124-3
- [9] Pruess, K., 1983. Heat transfer in fractured geothermal reservoirs with boiling. *Water Resources Research* 19 (1), doi:10.1029/WR019i001p00201
- [10] Mohais, R., Xu, C., Dowd, P., 2011. Fluid Flow and Heat Transfer Within a Single Horizontal Fracture in an Enhanced Geothermal System. *Journal of Heat Transfer* 133 (11), 112603-1 – 112603-8, doi:10.1115/1.4004369
- [11] Zhao, J., Tso, C.P., 1993. Heat transfer by water flow in rock fractures and the application to hot dry rock geothermal systems. *International Journal of Rock Mechanics & Mining Sciences* 30 (6), 633-641, doi:10.1016/0148-9062(93)91223-6
- [12] Li, Z.W., Feng, X.T., Zhang, Y.J., Zhang, C., Xu, T.F., Wang, Y.S., 2017. Experimental research on the convection heat transfer characteristics of distilled water in manmade smooth

and rough rock fractures. *Energy* 133, 206-218, doi:10.1016/j.energy.2017.05.127

[13] Bai, B., He, Y., Li, X., Li, J., Huang, X., Zhu, J., 2017. Experimental and analytical study of the overall heat transfer coefficient of water flowing through a single fracture in a granite core. *Applied Thermal Engineering* 116 (Complete), 79-90, doi:10.1016/j.applthermaleng.2017.01.020

[14] Ma, Y., Zhang, Y., Yu, Z., Huang, Y., Zhang, C., 2018. Heat transfer by water flowing through rough fractures and distribution of local heat transfer coefficient along the flow direction. *International Journal of Heat and Mass Transfer* 119, 139-147, doi:10.1016/j.ijheatmasstransfer.2017.11.102

[15] Zhao, Z., 2014. On the heat transfer coefficient between rock fracture walls and flowing fluid. *Computers and Geotechnics* 59, 105-111, doi:10.1016/j.compgeo.2014.03.002

[16] Barton, N., 1973. Review of a new shear-strength criterion for rock joints. *Engineering Geology* 7 (4), 287-332, doi:10.1016/0013-7952(73)90013-6

[17] He, R.H., Rong, G., Tan, J., Cheng, L., 2019. Numerical investigation of fracture morphology effect on heat transfer characteristics of water flow through a single fracture. *Geothermics* 82, 51-62, doi:10.1016/j.geothermics.2019.05.014

[18] Zhang, Z., Nemcik, J., Qiao, Q., Geng, X., 2015. A Model for Water Flow Through Rock Fractures Based on Friction Factor. *Rock Mechanics & Rock Engineering*, doi:10.1007/s00603-014-0562-4

[19] Luo, S., Zhao, Z., Peng, H., Hai, 2016. The role of fracture surface roughness in macroscopic fluid flow and heat transfer in fractured rocks. *International Journal of Rock Mechanics & Mining Sciences* 87, 29-38, doi:10.1016/j.ijrmms.2016.05.006

[20] Aliyu, M.D., Chen, H.P., 2017. Sensitivity analysis of deep geothermal reservoir: Effect of reservoir parameters on production temperature. *Energy* 129 (Jun.15), 101-113, doi:10.1016/j.energy.2017.04.091

[21] Bai, B., He, Y., Li, X., 2018. Numerical study on the heat transfer characteristics between supercritical carbon dioxide and granite fracture wall. *Geothermics* 75, 40-47, doi:10.1016/j.geothermics.2018.03.002

[22] Tse, R., Cruden, D.M., 1979. Estimating joint roughness coefficients. *International Journal of Rock Mechanics and Mining Sciences & Geomechanics Abstracts* 16 (5), 303-307, doi:10.1016/0148-9062(79)90241-9